An Area Segmentation Strategy for Adaptive Transmission to Achieve Near-Uniform High Quality Coverage in 30 GHz Fixed Wireless Cellular Systems in Tropical Regions

SUWADI, GAMANTYO HENDRANTORO, AND WIRAWAN

Department of Electrical Engineering
Institut Teknologi Sepuluh Nopember
Kampus ITS Sukolilo, Surabaya 60111,
INDONESIA
suwadi@ee.its.ac.id, gamantyo@ee.its.ac.id, wirawan@its.ac.id
http://www.its.ac.id

Abstract: This paper presents an area-segmented adaptive transmission strategy aiming at providing near-uniform high quality coverage in terms of availability and average spectral efficiency across the coverage area in broadband fixed wireless access (BFWA) systems operating at 30 GHz. The strategy considers implementation during rain in tropical regions with heavy rain rates of fixed 64-QAM, adaptive modulation (AM), adaptive coded modulation (ACM) with or without cell-site diversity with selection combining (SC), to be implemented in different ring-shaped segments around each base transceiver station (BTS). The results of synthetic storm-based evaluation show that near-uniform high quality coverage in tropical regions can be achieved using this strategy. Discussions are made upon the implementation of the area segmentation strategy in cellular configurations having square cells with different spacings between BTSs.

Key-Words: - Adaptive transmission, Coverage, Fixed wireless Cellular, Rain attenuation, Millimeter-wave

1. Introduction

The demand for broadband communication for high-speed high-quality multimedia transmission is driving the use of higher radio frequency spectrum. One of the systems that make use of such a high spectrum is the local multipoint distribution services (LMDS) which is a line of sight (LOS) point-to-multipoint wireless access system operating at millimeter-wave frequency [1]. LMDS is a broadband fixed wireless access system (BFWA) designed to deliver broadcast services (multimedia, video, internet, etc) from a central transmitter to individual subscriber terminals or CPEs (customer premise equipments) within its coverage area. In order to make efficient use of the spectrum, a cellular network configuration with multiple hubs or BTSs (base transceiver systems) can be applied. The frequency bands allocated by ITU-R and CEPT are usually above 20 GHz. In this band, rain attenuation is the most influential propagation factor to determine the system availability [2, 3].

At high rainfall intensities, the occurrence of which is of special interest in system requiring high-reliability links, the horizontal structure of rain is highly variable [2]. It is frequently observed that during a shower, high intensity rain is localized in a very small area surrounded by a region of more uniform, low intensity rain. Hence, in a cellular system under rain with localized storms, there is potential that a subscriber terminal receiving a heavily attenuated signal from one hub can obtain less attenuated, acceptable reception from another. This makes cell-site diversity a very promising method for improving link reliability and area coverage. The cell-site diversity technique has been proposed in order to reduce the outage time due to the above reason [4]-[6], including and especially in tropical countries where rainfall intensities are very high [7]. Evaluation of LMDS system performance in tropical rain conditions using cell-site diversity with various combining techniques, i.e. selection combining (SC) and maximum-ratio combining (MRC) has been studied by Suwadi et al. [8]. In addition, combined uses of several Rayleigh fading compensation techniques, i.e. power control, AM, ACM and diversity, have also been studied [9]. The method is able to improve link availability and maintain average capacity during rain.

Near-uniform high quality coverage is one of the design objectives of broadband cellular radio networks. While employing a combination of adaptive modulation, coding and cell-site diversity might maintain high quality access for a given subscriber terminal, it is also desired that subscribers located near the cell border experience as small degradation as possible in access quality with respect to those near the BTS. The access quality measures might include availability (in terms of error performance) and average capacity (or average spectral efficiency). To achieve the near-uniform coverage, different transmission schemes can be used for subscriber terminals at different distances from the BTS. For example, through analysis using rain measurements in Canada, Hendrantoro et al [4] proposed the use of cell-site diversity for subscriber terminals located around the corners and edges of square cells of a 30-GHz fixed cellular system. However, for a similar system implemented in tropical regions, the same strategy might not work as well.

This paper proposes a strategy to achieve near-uniform coverage in terms of availability and spectral efficiency in a 30-GHz fixed cellular system with square cells in a tropical rain climate. The strategy is implemented by segmenting the area surrounding a BTS into rings, in each of which a certain combination of adaptive modulation, coding, and cell-site diversity is used. The proposed strategy is designed following the results of simulation study evaluating link availability and average spectral efficiency using fixed 64 QAM, AM (adaptive modulation), ACM (adaptive coded modulation), SC (cell-site diversity with selection combining), joint AM-SC and joint ACM-SC. The evaluation is done by applying the synthetic storm technique (SST) based on rainfall intensities measurement in Surabaya, Indonesia, and adopting ITU-R P.530 recommendation for calculating rain attenuation [10].

Following this introductory section, we describe the characteristics of tropical rain attenuation estimates obtained through synthetic storm technique (SST) applied to rain rate measurements and show that the results do not fit the commonly assumed lognormal distribution. Accordingly, in subsequent sections, the analysis is made on the basis of the SST results instead of the lognormal assumption commonly adopted in studies of millimeter-wave applications in non-tropical regions. Section III describes the system model, which include the AM, ACM and SC, as well as the cell plan and system parameters. In section IV, a performance evaluation of link availability and spectral efficiency is reported, the results of which are then applied to the cell plan to produce the desired area segmentation scenario for a given cell size. Finally, a summary is given in the last section.

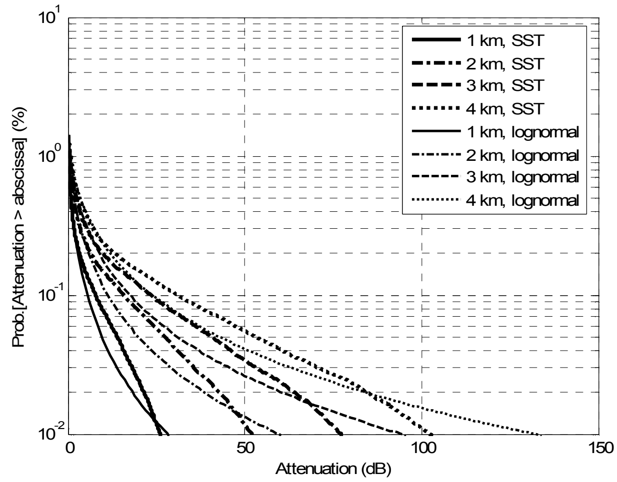

Fig. 1 CCDFs of rain attenuation for single link with 1-4 km link lengths

2. Rain Attenuation Characteristics

Rain attenuation was estimated from rain rate time series by invoking the synthetic storm technique (SST). The SST had previously been tested successfully by Matricciani [11] for predicting conventional long term statistics of fade duration and long term relative to contiguous periods of the day of four hours. For each rainstorm, the SST can generate a rain attenuation time series at any carrier frequency and polarization from a corresponding rain rate time series by using wind velocity measurement.

A disdrometer has been placed on the rooftop of the Electrical Engineering Department building in the campus of Institut Teknologi Sepuluh Nopember in Surabaya, Indonesia (7°13' S, 112°43' E) since 2007 to measure rain rate time series [12]. Our study uses 2 years of rain rate measurement data. Surabaya's weather is typical of maritime tropical regions. Based on the rain attenuation estimates, we can obtain mean μ and standard deviation σ of the logarithm of rain attenuation.

It is generally accepted that rain attenuation value A (dB) is approximately log-normally distributed. Therefore, the overall long-term probability density function (pdf) of rain attenuation along the link has the form: [13]

$$p_A(a) = \begin{cases} \dfrac{1}{a\sigma\sqrt{2\pi}} \exp\left(-\dfrac{1}{2}\left[\dfrac{\ln a - \mu}{\sigma} \right]^2 \right), & a \geq 0 \\ 0, \quad a < 0 \end{cases} \tag{1}$$

and the CCDF (complementary cumulative distribution function):

$$P(A \geq a) = \int_a^\infty p_A(\lambda)d\lambda = Q\left(\frac{\ln(a) - \mu}{\sigma}\right) \quad (2)$$

where μ and σ are the mean and standard deviation of $\ln(A)$.

Fig. 1 compares CCDFs of rain attenuation obtained using SST and those obtained analytically using the log-normal assumption. It can be seen that the SST results cannot be approximated well by the analytical ones, especially for longer links. The analytical lognormal CCDF tends to underestimate that of the SST result, except for values around exceedance probability of 0.01% for which the log-normal tends to overestimate the SST. This might lead to inaccuracies in performance evaluation later on, which requires either the average or the 99.99-th percentile statistics of the performance indicators. Hence, in the subsequent study we would not adopt the log-normal assumption, and instead, use rain attenuation estimates obtained from the SST method.

In the presence of rain attenuation, the received signal-to-noise power ratio γ is given by

$$\gamma = \gamma_{cs} 10^{-A/10} \quad (3)$$

where γ_{cs} and A are signal-to-noise power ratio in clear sky condition in linear scale and rain attenuation in dB, respectively. The effects of interference have been shown to be neglectable, especially so during rain [13], and hence are not considered in this study.

3. System Model

To cope with the variation in link attenuation due to rain, the system under consideration employs five transmission schemes, namely, fixed 64-QAM, AM (adaptive modulation without coding), ACM (adaptive coded modulation), AM-SC (adaptive modulation with cell-site selective combining diversity) and ACM-SC (adaptive coded modulation with cell-site diversity). In clear sky conditions, the channel is only affected by Gaussian noise with power spectral density N (W/Hz) and the co-channel co-polar interferences, and hence the system uses 64-QAM to achieve maximum spectral efficiency of 6 bps/Hz with 100% availability. The availability of channel state information (in the form of SNR experienced by the user receiver) at the BTS transmitter allows it to adapt its transmission scheme with respect to the channel gain. The feedback channel can take the form of a radio channel at a frequency sufficiently low to preclude the destroying impact of rain attenuation. Since each of the adaptive scheme employs only four different modes, as we shall see later, the feedback information requires only two bits. We ignore the effects of feedback delay since in reality this delay is very small with respect to the rate of variation of rain attenuation. In the following, we discuss the modes used within the schemes and relevant issues, including the cellular network configuration.

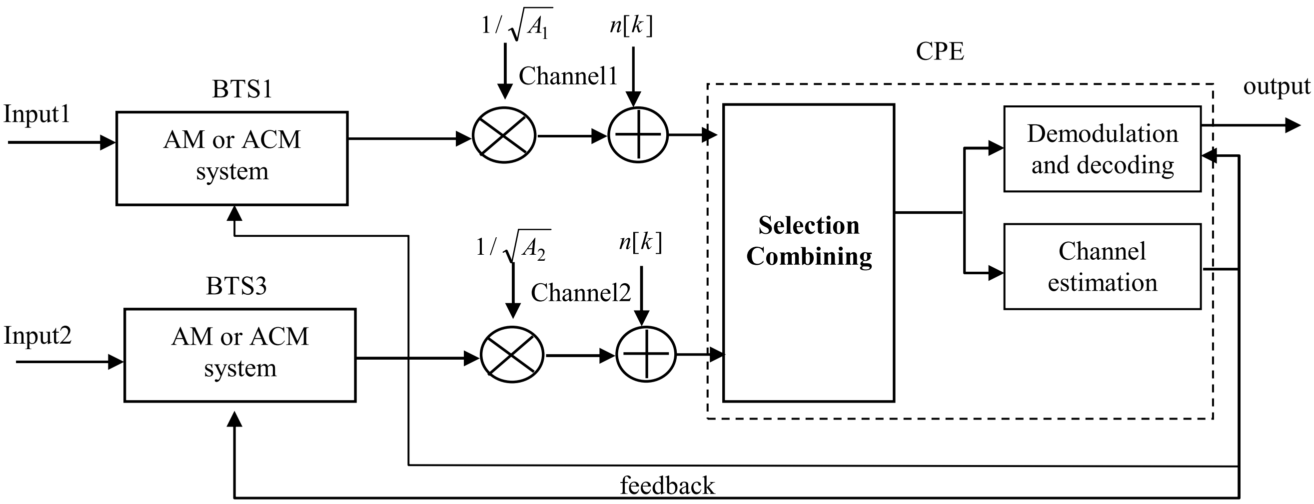

Fig. 2 AM, ACM and SC on BFWA system.

Table 1 AM scheme scenario for maximum $P_b = 10^{-6}$

Region (j)	**Mode**	M_j	γ **Interval (dB)**
0	No transmission	0	$\gamma < 13.88$
1	4 QAM	4	$13.88 < \gamma < 20.87$
2	16 QAM	16	$20.87 < \gamma < 27.10$
3	64 QAM	64	$\gamma > 27.10$

A. Adaptive Modulation

For the adaptive modulation technique, shown diagramatically in Fig. 2, we assume perfect channel estimation and error-free feedback path. The transmitters belong to two BTSs, referred to as BTS 1 and 3 in the figure following the scenario adopted in later sections involving four corner BTSs serving a square area operating in diversity with respect to the CPE (see Fig. 3). The system uses various modulation levels or modes, i.e., 4, 16 and 64-QAM, each applied to the appropriate channel condition. In clear-sky conditions, the system is in the 64-QAM mode. However, in rain conditions, the channel is affected by rain attenuation which causes the received signal-to-interference and noise power ratio γ to decrease, so the system has to use lower modulation level, i.e., 16-QAM or 4-QAM.

Probability of bit error of the M-QAM system can be obtained as follows:

$$P_b = \frac{2}{\log_2 M}\left\{\frac{\sqrt{M}-1}{\sqrt{M}}\right\}\left[1 - erf\sqrt{\frac{3T_0 B}{2(M-1)}(\gamma)}\right] \quad (4)$$

where M and γ are modulation level and signal-to-noise power ratio, respectively. The value of T_0B is assumed to be unity. Adaptation scenario based on γ for maximum bit error rate of 10^{-6} for AM is shown in Table 1.

To assess the average capacity provided by the adaptive modulation method, the channel capacity as defined by Shannon [9] is chosen since it gives the maximum rate of transmission signal over the channel. If the channel is subject to fading, its capacity varies with the changes in the propagation medium. Average spectral efficiency in bps/Hz of Adaptive M-QAM system can hence be calculated as follow:

$$\frac{C}{B} = \sum_{i=1}^{N} \log_2(M_i).P(M_i) \quad (5)$$

where M_i, $P(M_i)$, and N denote modulation level of the i-th mode, probability of the i-th mode and number of modes, respectively.

B. Adaptive Coded Modulation

While the addition of coding can increase link availability, it also reduces spectral efficiency. As before, the system uses M-QAM with various modulation levels, the selection of which depends on channel condition. On top of that, a concatenation of a convolutional code CC(k/n) and Reed Solomon code RS(n, k) is employed. Bit error probability calculation of the system using adaptive code modulation with CC (k/n) and RS (n, k) code in clear sky condition can be obtained as follows: [14],[15]

$$P_b \approx \left(\frac{1}{2^m - 1}\sum_{j=t+1}^{2^m-1} j\binom{2^m-1}{j} Pe_{cc}\, j(1-Pe_{cc})^{2^m-1-j}\right) \times \log_2 M \quad (6)$$

where m, t, M and Pe_{cc} are the number of bits represented by a symbol, symbol error correcting capability of the RS code, modulation level and symbol error probability after the use of convolutional code, respectively. The latter can be expressed as follows:

$$Pe_{cc} = \begin{cases} \left(\frac{1}{k}(1.06)^{d_{free}} A_{d_{free}} \exp\left(-\frac{r d_{free}\gamma}{2}\right)\right)\log_2 M, \\ for \quad M = 4 \\ \left(\frac{1}{k}(0.92)^{d_{free}} A_{d_{free}} \exp\left(-\frac{r d_{free}\gamma}{5}\right)\right)\log_2 M, \\ for \quad M = 16 \\ \left(\frac{1}{k}(0.8)^{d_{free}} A_{d_{free}} \exp\left(-\frac{r d_{free}\gamma}{7}\right)\right)\log_2 M, \\ for \quad M = 64 \end{cases} \quad (7)$$

Table 2 ACM scheme scenario for maximum P_b =10^{-6}

Region (j)	**Mode**	M_j	γ **Interval (dB)**
0	No transmission	0	$\gamma < 1.18$
1	4 QAM+RS(63,31)+CC(1/3)	4	$1.18 < \gamma < 11.45$
2	16 QAM+RS(63,51)+CC(1/2)	16	$11.45 < \gamma < 21.63$
3	64 QAM+RS(63,59)+CC(2/3)	64	$\gamma > 21.63$

where d_{free}, r, k, $A_{d_{free}}$ and γ are free distance, convolutional code rate, bits information per codeword, number of codewords having free distance d_{free} from the all-zero codeword and signal to-noise ratio respectively. By using equations (6) and (7), we can obtain thresholds of signal-to-noise power ratio γ at the receiver for determining modulation level. Adaptation scenario based on γ for maximum bit error probability of 10^{-6} for ACM is shown in Table 2.

The average spectral efficiency in bps/Hz of the ACM system can be calculated as follow:

$$\frac{C}{B} = \sum_{i=1}^{N} \log_2(M_i).P(M_i).\frac{k_{cc_i}}{n_{cc_i}}.\frac{k_{RS_i}}{n_{RS_i}} \qquad (8)$$

where $\frac{k_{cc_i}}{n_{cc_i}}, \frac{k_{RS_i}}{n_{RS_i}}$ are respectively the number of information bit-to-code word ratio of convolutional code and Reed-Solomon code in the i-th mode.

C. Cell Site Diversity

Recently, there were three combining techniques considered for use in diversity technique to mitigate rain fading, i.e. SC, EGC and MRC [9]. In this study, we choose to use SC because it has the simplest circuit and consumes the least power and spectral resources of the BTSs. In our system, the cell-site diversity configuration involves two approximately opposite base stations with respect to the user terminal considered. The selection combining in the receiver at a user terminal selects the signal with better SNR from the two base sttations. In reality, the two signals used to determine the selection can take the form of pilot signals. Output signal-to-noise power ratio of SC is

$$\gamma_{SC} = \max\{\gamma_1;\gamma_2\} \qquad (9)$$

where, γ_n is signal-to-interference and noise power ratio of the n-th link. It should be noted here that the adoption of cell-site diversity might somewhat complicate the implementation due to the requirement for the user terminal to monitor continually the quality of the other link, particularly when it rains, and for the system to quickly respond to the request to switch the link.

D. System Parameters and Cell Planning

The 30 GHz cellular network is assumed to include multiple base transceiver stations (BTSs) as well as subscriber terminals or customer premise equipments (CPEs). The BTS transmitter is of 0 dBW power, whereas a receiver with a thermal noise power density at the input to detector of -138.86 dBW/MHz is employed at the CPE. The antenna main lobe is assumed to have a Gaussian characteristic with quadratically decreasing gain in dBi [16]:

$$G(\theta) = G_{\max} - 3(\theta/\theta_{3dB})^2 \qquad (10)$$

where $G(\theta)$, $G_{\max}$ and θ_{3dB} are respectively antenna gain in azimuth angle θ, maximum antenna gain, and the angle of 3-dB decrease of antenna gain from the maximum (i.e., half of the 3-dB beamwidth). The BTS antenna is a 90^o 3-dB beamwidth sectoral and of maximum gain of 20.15 dB, whereas CPE antenna has a 5^o 3-dB beamwidth and maximum gain of 34.96 dB. These are typical parameter values used in a fixed broadband wireless access (BWA) [13].

The system is assumed to adopt cellular configuration with square cells, each having four 90^o sectors. Fig. 3 shows a square area with a BTS at each of its corner. This represents an area consisting of four sectors of four neighbouring cells. The length of each side of this area represents the spacing between adjacent BTSs. The cell plan with 4 sectors is pertinent with 4 channels, which can be realized as a combination of two frequencies and two polarizations. BTS1 (the main BTS) and BTS3 (the diagonal opposite) can operate in diversity whenever required. In our simulation, we investigate various locations of CPEs in the sector served by BTS1.

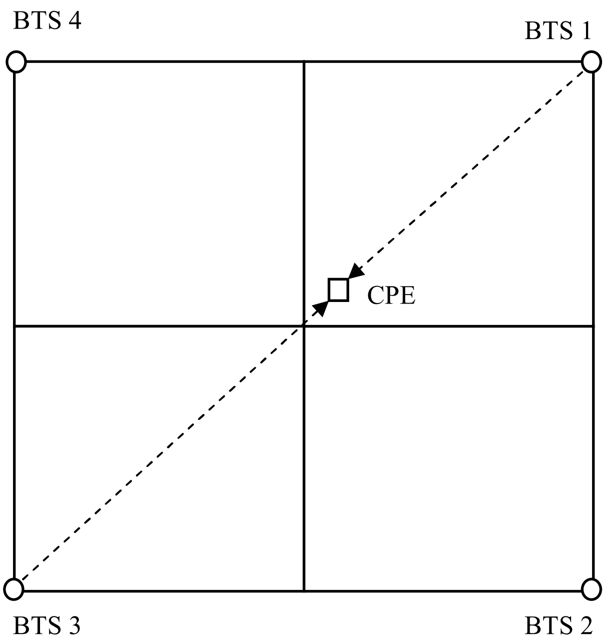

Fig. 3 A square area with four corner BTSs

4. Simulation Results and Discussion

Link availability with respect to a maximum bit error probability of 10^{-6} and average spectral efficiency for CPEs at various locations (and distances from the main BTS) were evaluated for systems with fixed 64-QAM, AM, ACM, AM-SC and ACM-SC. The order of reference above shows an increasingly complex implementation. The results of simulation for each scheme are shown in Table 3 and 4. It can be seen that fixed 64-QAM is sufficient for use by CPEs located not further than 1 km from the serving BTS to achieve availability and average spectral efficiency greater than 99.99% and 5.999 bps/Hz, respectively. Later on we will refer to the area occupied by these users as Segment I.

For CPEs located between 1 and 2 km away from the BTS, the area that we refer to as Segment II, maintaining fixed 64-QAM results in availability of 99.93%. If minimum availability of 99.95% is desired, than fixed 64-QAM is certainly not the best choice. Instead, we can choose AM, which achieves at least 99.97% availability and undergoes only a small degradation in average spectral efficiency.

For the area ranging from 2 to 3 km away from the BTS, namely, Segment III, there are two options that can be opted for to achieve 99.95% minimum availability, that is, ACM and AM-SC. Each has its own disadvantages; ACM yields much lower average spectral efficiency due to the concatenated coding incorporated to boost the error rate performance, whereas the AM-SC requires diversity operation between two BTSs that increase the complexity and resources consumption of the system. Hence, in this case, the choice is governed by consideration of the importance between high capacity and lower complexity.

Table 3 Simulation results of link availability (%) for various location CPE_s from main BTS in the presence of rain fading

Transmission Scheme	Link length and Segment Index			
	d < 1 km, Segment I	**1 <d< 2 km, Segment II**	**2 <d< 3 km, Segment III**	**3 <d< 4 km, Segment IV**
Fixed 64-QAM	**99.99**	99.93	99.87	99.82
AM	**99.99**	**99.97**	99.93	99.88
ACM	**99.99**	**99.98**	**99.96**	99.93
AM-SC	**99.99**	**99.97**	**99.96**	**99.95**
ACM-SC	**99.99**	**99.99**	**99.98**	**99.97**

Table 4 Simulation results of spectral efficiency (%) for various location CPE_s from main BTS in the presence of rain fading

Transmission Scheme	Link length and Segment Index			
	d < 1 km, Segment I	**1 <d< 2 km, Segment II**	**2 <d< 3 km, Segment III**	**3 <d< 4 km, Segment IV**
Fixed 64-QAM	5.999	5.996	5.992	5.989
AM	5.999	5.997	5.994	5.992
ACM	3.746	3.745	3.743	3.742
AM-SC	5.999	5.998	5.997	5.995
ACM-SC	3.746	3.745	3.744	3.744

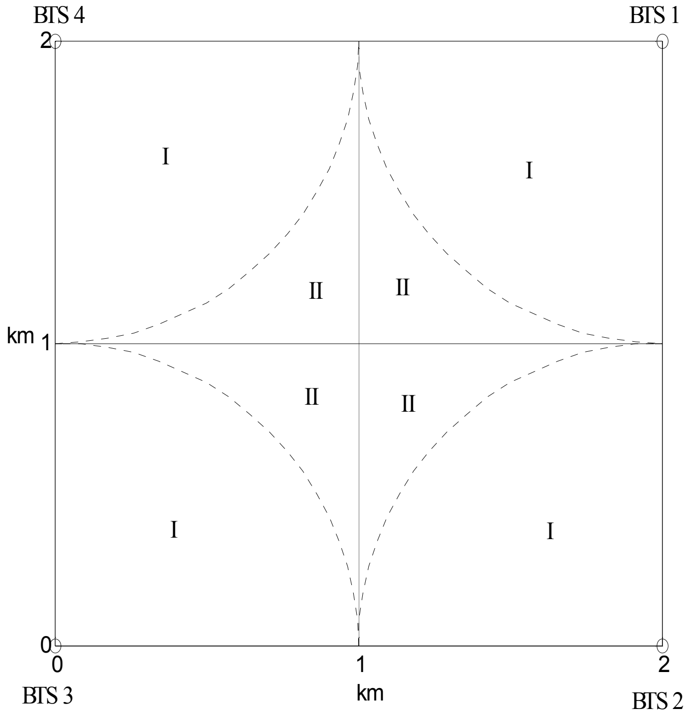

Fig. 4 Cell Plan 1 for systems with 2 km spacing between neighbouring BTSs.

Table 5 Area segmentation of adaptive transmission schemes for configuration with 2 km cell spacing

Segment	Percent of Coverage Area (%)	Transmission Scheme	Link Availability (%)	Average Spectral Efficiency (Bps/Hz)
I	78.57	Fixed 64-QAM	99.99	5.999
II	21.43	AM	99.97	5.997

Finally, for CPEs located within Segment IV ranging from 3 to 4 km from the BTS, there are also two choices available, namely, AM-SC and ACM-SC. The choice perhaps tends toward joint AM-SC rather than joint ACM-SC, due primarily to the much higher average capacity, similar complexity and only slightly lower availability that is still 99.95% in the least.

We observe that the division of cell area following the above segmentation in a location with tropical rain characteristics as described in Section 2 will result in availability of more than 99.95% almost anywhere in the coverage area. For example, according to Tables 3 and 4, CPEs located in Segment I employ 64 QAM and consequently achieve at least 99.99% link availability and 5.999 bps/Hz average spectral efficiency. Those in Segment II use AM with availability higher than 99.97% and average capacity of 5.997 bps/Hz. Using these results we will examine area segmentation within the square for three different spacings between adjacent BTSs. In particular, Cell Plan 1 represents a square area of a configuration with 2 km BTS spacing, Cell Plan 2 represents that with 4 km spacing and Cell Plan 3 with 6 km spacing.

For the system with small cells having only 2 km spacing between BTSs as represented by Cell Plan 1, each sector is divided into two segments, I and II, separated by rings centered at the corner BTSs as shown in Fig. 4. Within each sector, a certain transmission scheme is employed, as presented in Table 5. Segment I, in which fixed 64-QAM is used, constitutes 78.57% of the whole area, whereas Segment II that employs AM constitutes the remaining 21.43%. The area percentage might translate to the approximate percentage of users in the segment if the users are assumed to be distributed uniformly in the area, which means only about 21.43% of the users that are required to adopt AM. This is a relatively simpler scenario compared to those with larger spacing between BTSs as can be seen later. However, with such a small spacing, it requires deployment of a large number of BTSs for a specific targeted service area of an operator.

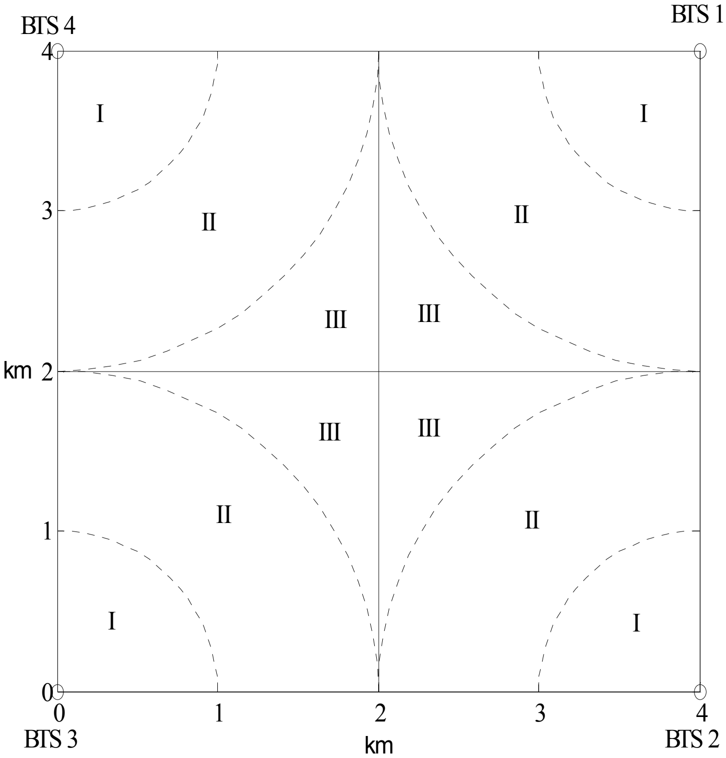

Fig. 5 Cell Plan 2 for systems with 4 km spacing between neighbouring BTSs.

Table 6 Area segmentation of adaptive transmission schemes for configuration with 4 km cell spacing

Segment	Percent of Coverage Area (%)	Transmission Scheme	Link Availability (%)	Average Spectral Efficiency (Bps/Hz)
I	19.64	Fixed 64-QAM	99.99	5.999
II	58.93	AM	99.97	5.997
III	21.43	ACM or AM-SC	99.96	3.743 or 5.997

For the system with 4 km BTS spacing, i.e., Cell Plan 2 as given in Fig. 5, each sector is segmented into three concentric quarter rings, that is, Segments I–III. Within each of these segments a certain transmission scheme is employed, as shown in Table 6. In Segments I and II, fixed 64-QAM and AM are used, respectively. However, as previously discussed, we are faced with a choice between ACM and AM-SC for Segment III. As before, the choice depends on which of the two criteria, average spectral efficiency and complexity, is considered more crucial. In this cell plan, Segments I to III each constitute 19.64%, 58.93% and 21.43% of the whole area, respectively, and might translate straightforwardly into percentage of CPEs if uniform distribution of CPEs is assumed. It can be observed that the majority of the users will have to use AM.

As the last exemplary cell plan, we examine Cell Plan 3, in which neighbouring BTSs are separated by 6 km spacings as shown in Fig. 6. In this case, the cell area is divided into five segments. Segments I to V each constitute 8.73%, 26.18%, 43.63%, 20.76% and 0.70% of the whole area. The transmission scheme assigned to each segment is given in Table 7. Schemes used in Segments I-III are as in the previous cell plans. For Segment IV, we are again faced with two choices as previously discussed, with AM-SC being the preferred scheme. A few more CPEs in Segment V might require the use of joint ACM-SC to maintain the high availability in the expense of average capacity, or AM-SC if the 0.7% users in this segment do not mind to have a slightly lower availability than 99.95%. Segment III and IV can be combined into an area of 64.39%, if the system uses joint AM-SC. If we can afford the complexity of diversity, then for a system with 6 km spacing between adjacent BTSs it is better to use joint AM-SC in Segments III, IV and V to achieve the best possible performance in terms of link availability and average spectral efficiency.

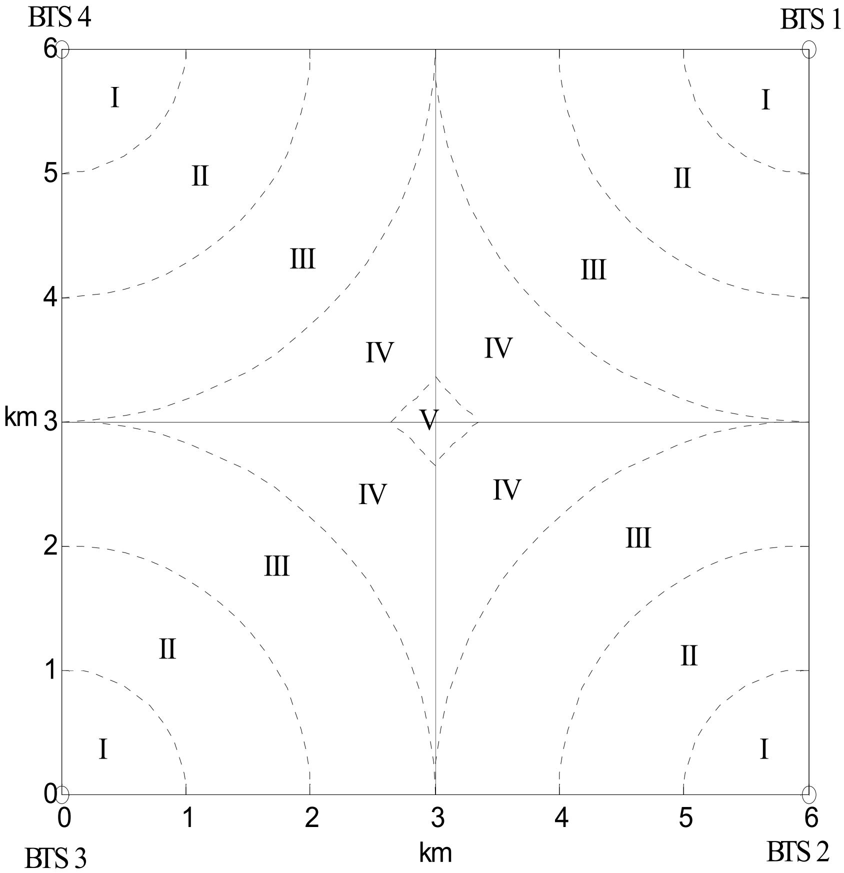

Fig. 6 Cell Plan 3 for systems with 6 km spacing between neighbouring BTSs.

Table 7. Area segmentation of adaptive transmission schemes for configuration with 6 km cell spacing

Segment	Percentage of Coverage Area (%)	Transmission Scheme	Link Availability (%)	Average Spectral Efficiency (Bps/Hz)
I	8.73	Fixed 64-QAM	99.99	5.999
II	26.18	AM	99.97	5.997
III	43.63	ACM or AM-SC	99.96	3.743 or 5.997
IV	20.76	AM-SC	99.95	5.995
V	0.7	ACM-SC	99.95	3.744

In comparing the three cell plans, one might also consider that a network serving a region with dense or moderately dense population might benefit from smaller cells since the deployment of more BTSs is justified by the higher traffic density, and hence the use of a simpler transmission system is preferred. In contrast, for regions of low population density the use of larger cells or smaller number of BTSs might be justifiable, while relatively fewer users allow for more complex schemes.

5. Conclusion

We have outlined a strategy to achieve high quality performance almost uniformly across the coverage area of a BFWA system in tropical rain regions based on segmentation of the area into concentric rings and application of adaptive transmission techniques. In particular, minimum availability of 99.95% can be achieved for maximum bit error rate of 10^{-6} in tropical regions by using one of four possible adaptive schemes in each of the outer rings.

We have also learnt that to implement the system with small square cells, i.e., having 2 km spacing between BTSs, it is sufficient to divide the coverage area into two segments and to use fixed 64 QAM in the inner segment and adaptive modulation in the outer, a strategy suitable for urban and metropolitan areas with high subscriber density. On the other hand, systems with BTS spacing of 4 km and 6 km, requiring area division into three or more ring segments and use of more complex adaptive transmission strategy, are more suitable for areas with more sparse population.

The proposed strategy is especially worthwhile for use in tropical regions, but probably not so for non-tropical. In addition, while herein the strategy is designed specifically for the 30 GHz band, the area segmentation method in general might be useful for other bands above 10 GHz, requiring the process outlined in this paper to determine the segmentation scheme and the associated adaptive transmission modes. Finally, it should also be pointed out that our study only considers transmission using conventional single carrier scheme, and hence, a slightly further study might be necessary for systems using multi-carrier schemes such as OFDM.

Acknowledgement
This work was financially supported by a Doctoral Research Grant from the Indonesian government. Mr. Suwadi's study was supported by a BPPS scholarship from the government.

References
[1] C. Smith, *LMDS*, New York: McGraw-Hill, 2000.
[2] R.K. Crane, *Electromagnetic Wave Propagation Through Rain*: New York, Wiley, 1996.
[3] A. Paraboni, G. Masini, and A. Elia, "The effect of precipitation on microwave LMDS networks-performance analysis using a physical rain cell model", *IEEE J. Selected Areas Comm*,. Vol. 20, April 2002, pp. 615-619.
[4] G. Hendrantoro, R.J.C. Bultitude, and D.D. Falconer, "Use of cell-site diversity in millimeter-wave fixed cellular systems to combat the effects of rain attenuation", *IEEE J. Select. Areas Commun*., vol. 20, Apr. 2002, pp. 602-614.
[5] A.D. Panagopoulos and J.D. Kanellopulos, "Cell-site diversity performance of millimeter-wave fixed cellular systems operating at frequencies above 20 GHz ", *IEEE Antennas and Wireless prop. Letter*, vol.1, 2002, pp. 183-185.
[6] G. C. Dipiazza, "LMDS system having cell-site diversity and adaptability", *patent number: 6,141,557*, Oct., 31, 2000.
[7] A. Mauludiyanto, G. Hendrantoro, M.H. Purnomo, T. Ramadhany and A. Matsushima, "ARIMA modelling of tropical rain attenuation on a short 28-GHz terrestrial link", *IEEE Antennas and Wireless prop. Letter,* Vol.9, 2010, pp. 223-227.
[8] Suwadi, G. Hendrantoro, Wirawan, "Performance of Various Combining Techniques and Adaptive Coded Modulation in Millimeter-Wave Fixed Cellular Systems under the Impact of Rain Attenuation in Indonesia", *Proc. Asia Pacific Microwave Conference (APMC)*, Singapore, December 7-10, 2009.
[9] A. Goldsmith, "*Wireless Communications*", Cambridge University Press, 2005.
[10] ITU-R Rec. P.530-10, "*Propagation data and prediction methods required for the design of terrestrial line of sight systems*", 2001.
[11] E. Matricciani, "Service oriented statistics of interruption time due to rainfall in earth-space communication systems" *IEEE Transaction on antennas and propagation*, vol. 52, No. 8 August, 2004, pp. 2083-2089.
[12] G. Hendrantoro, A. Mauludiyanto, and P. Handayani, "A Measurement System for Space-Time Variation of Rainfall Rate and Millimeter-Wave Specific Attenuation in Indonesia", *Proc. Asia Pacific Microwave Conference (APMC)*, Japan, December, 2006
[13] C. Y. Chu, K. S. Chen, "Effects of Rain Fading on the Efficiency of the Ka-Band LMDS System in the Taiwan Area", *IEEE Transactions on Vehicular Technology*, vol. 54, no. 1, Januari 2005, pp. 9-19.
[14] B. Sklar. "*Digital Communication*", Prentice Hall, New Jersey, 1994.
[15] S. Haykin, "*Digital Communications*", John Wiley & Sons, 1988.
[16] E. Lutz, M. Werner, A. Jahn, "Satellite Systems for Personal and Broadband Communications", Springer, 2000.

Suwadi was born on August 18, 1968, in Gresik, Indonesia. He received the B.Eng. degree in electrical engineering from Institut Teknologi Sepuluh Nopember (ITS) Surabaya, Indonesia, in 1992, and M.Eng degree in electrical engineering from Insitut Teknologi Bandung (ITB), Indonesia, in 1999. He is currently working toward the Ph.D. degree in electrical engineering from ITS. He has presented four papers in national and three papers in international conferences. He received two best paper awards in international conferences. He has also published two papers in Indonesian journals.

Since 1993, he was as lecturer with the Department of Electrical Engineering, ITS. His research interests include digital communications, digital signal processing and broadband wireless communications.

Gamantyo Hendrantoro received the B.Eng degree in electrical engineering from Institut Teknologi Sepuluh Nopember (ITS), Indonesia, in 1992, and the MEng and PhD degrees in electrical engineering from Carleton University, Canada, in 1997 and 2001, respectively. He is presently a Professor with ITS.

His research interests include radio propagation modeling and wireless communications. He has recently been engaged in various collaborative studies, including investigation into millimeter-wave wireless systems for tropical areas with Kumamoto University, Japan, implementation of digital TV systems with BPPT, Indonesia, and development of Indonesia's first educational nano-satellite (IINUSAT) together with five other universities and LAPAN.

Dr. Hendrantoro is a Member of the IEEE.

Wirawan received the B.E. degree in telecommunication engineering from Institut Teknologi Sepuluh Nopember (ITS), Surabaya, Indonesia, in 1987, the DEA in signal and image processing from Ecole Supérieure en Sciences Informatiques, Sophia Antipolis, and the Dr. degree in image processing from Telecom ParisTech (previously Ecole Nationale Supérieure des Télécommunications), Paris, France, in 1996 and 2003, respectively.

Since 1989 he has been with ITS as lecturer in the Electrical Engineering Department. His research interests lie in the general area of statistical signal processing, and recently focuses more on underwater acoustic communication and networking and on various aspects of wireless sensor networks. He is a Member of IEEE.